PNAS RESEARCH ARTICLE | MEDICAL SCIENCES

HIV post-treatment controllers have distinct immunological and virological features

Behzad Etemad[a,1], Xiaoming Sun[b,1,2], Yijia Li[a,1,3], Meghan Melberg[a], Daniela Moisi[c], Rachel Gottlieb[a], Hayat Ahmed[a], Evgenia Aga[d], Ronald J. Bosch[d], Edward P. Acosta[e], Yuko Yuki[f,g], Maureen P. Martin[f,g], Mary Carrington[b,f,g], Rajesh T. Gandhi[h], Jeffrey M. Jacobson[c], Paul Volberding[i], Elizabeth Connick[j], Ronald Mitsuyasu[k], Ian Frank[l], Michael Saag[e], Joseph J. Eron[m], Daniel Skiest[n], David M. Margolis[m], Diane Havlir[i], Robert T. Schooley[o], Michael M. Lederman[c], Xu G. Yu[b], and Jonathan Z. Li[a,4]

Edited by John Coffin, Tufts University, Boston, MA; received November 12, 2022; accepted February 6, 2023

HIV post-treatment controllers (PTCs) are rare individuals who maintain low levels of viremia after stopping antiretroviral therapy (ART). Understanding the mechanisms of HIV post-treatment control will inform development of strategies aiming at achieving HIV functional cure. In this study, we evaluated 22 PTCs from 8 AIDS Clinical Trials Group (ACTG) analytical treatment interruption (ATI) studies who maintained viral loads ≤400 copies/mL for ≥24 wk. There were no significant differences in demographics or frequency of protective and susceptible human leukocyte antigen (HLA) alleles between PTCs and post-treatment noncontrollers (NCs, n = 37). Unlike NCs, PTCs demonstrated a stable HIV reservoir measured by cell-associated RNA (CA-RNA) and intact proviral DNA assay (IPDA) during analytical treatment interruption (ATI). Immunologically, PTCs demonstrated significantly lower $CD4^+$ and $CD8^+$ T cell activation, lower $CD4^+$ T cell exhaustion, and more robust Gag-specific $CD4^+$ T cell responses and natural killer (NK) cell responses. Sparse partial least squares discriminant analysis (sPLS-DA) identified a set of features enriched in PTCs, including a higher $CD4^+$ T cell% and $CD4^+/CD8^+$ ratio, more functional NK cells, and a lower $CD4^+$ T cell exhaustion level. These results provide insights into the key viral reservoir features and immunological profiles for HIV PTCs and have implications for future studies evaluating interventions to achieve an HIV functional cure.

HIV | analytical treatment interruption | post-treatment controller | reservoir | T cell

Significance

On most occasions, interruption of a stable antiretroviral therapy would lead to significant HIV viremia rebound. HIV post-treatment controllers (PTCs) are a rare group of people with HIV (PWH) who are able to control their rebound HIV to a very low level during analytical treatment interruption (ATI). It is important to understand the mechanisms behind this phenomenon. In this study, we revealed several important viro-immunological features associated with post-treatment control, and these findings can shed light on future HIV cure studies.

Strategies that can induce sustained HIV remission without antiretroviral therapy (ART) remain an elusive goal (1, 2). Therapeutic approaches to control HIV replication in the absence of ART require alternatives to the traditional model of HIV therapeutics. There have been reports of HIV remission with the use of hematopoietic stem cell transplantation (3, 4), but such a strategy carries significant toxicity and mortality risk that precludes its adoption into general clinical care. The existence of HIV elite controllers (ECs) indicates that the goal of ART-free HIV remission is possible, but ECs frequently have favorable genetic profiles (5) that are not easily translatable to the development of therapeutics.

Post-treatment controllers (PTCs) may serve as a more tangible goal for studies aimed at achieving HIV ART-free remission. While the majority of people with HIV (PWH) experience viral rebound within 4 wk of ART discontinuation (6–8), there are rare individuals who demonstrate sustained virological suppression for months or years after an analytical treatment interruption (ATI) (9–12). In the Control of HIV after Antiretroviral Medication Pause (CHAMP) study, we described a cohort of HIV PTCs identified in several AIDS Clinical Trials Group (ACTG) ATI studies and other cohort studies (13). We found that early initiation of ART increased the chances of post-treatment control but that PTCs could also be identified in those who initiated ART during chronic infection. The CHAMP study represents the largest PTC cohort to date, but which host and virological factors are associated with post-treatment control remains understudied. To this end, we performed an in-depth evaluation of the genetic, virological, immunological, and inflammatory characteristics of these PTCs compared to a group of post-treatment noncontrollers (NCs) who demonstrated rapid viral rebound after an ATI. The identification of characteristics associated with post-treatment virological control may lead to the recognition of PTC candidates prior to ART discontinuation and targeted mechanistic studies that could inform development of therapeutic strategies for HIV remission.

Results

Baseline Characteristics and Viral Load Trajectory. We included 59 participants with available stored samples in this analysis, including 22 PTCs and 37 NCs from ACTG ATI studies. Baseline age, sex, race, duration of ART, and percentage who initiated ART during

Competing interest statement: J.Z.L has received research support from Merck. M.M.L. and X.G.Y have received research support from Gilead Sciences. I.F. has received honoraria as a consultant to Gilead Sciences, ViiV Healthcare, and Merck and has received research support from Janssen Therapeutics, Sanofi, Moderna, and Pfizer. The content of this publication does not necessarily reflect the views or policies of the Department of Health and Human Services, nor does mention of trade names, commercial products, or organizations imply endorsement by the US Government.

This article is a PNAS Direct Submission.

[1]B.E., X.S., and Y.L. contributed equally to this work.

[2]Present address: Key Laboratory of Aging and Cancer biology, Department of Immunology and Pathogen Biology, School of Basic Medical Sciences, Hangzhou Normal University, Zhejiang, China 311121.

[3]Present address: Department of Medicine, University of Pittsburgh, Pittsburgh, PA 15213.

[4]To whom correspondence may be addressed. Email: jli@bwh.harvard.edu.

This article contains supporting information online at https://www.pnas.org/lookup/suppl/doi:10.1073/pnas.2218960120/-/DCSupplemental.

Published March 6, 2023.

early/acute infection were comparable between the PTC and NC groups (*SI Appendix*, Table S1). Approximately 30% of the PTC and NC participants received an experimental intervention (primarily a therapeutic vaccine) prior to the ATI per the parent study protocols (*SI Appendix*, Table S2).

First, we compared the viral load (VL) trajectory during ATI in PTCs and NCs. As expected, PTCs and NCs experienced different levels of viral rebound, with NCs having a higher peak VL (PTCs vs. NCs: 2.5 vs. 4.3 $\log_{10}$ copies/mL), although VL peaked before post-ATI week 10 in both groups (Fig. 1*A*). VL subsequently declined to the set point between weeks 10 and 25 and fluctuated around the set point until ART was resumed or the end of follow-up (Fig. 1*A*). When stratified by the duration of HIV infection before ART initiation, acute/early-treated PTC and NC participants followed a similar trajectory of viral rebound as the chronic-treated participants (*SI Appendix*, Fig. S1*A*). A subgroup of participants had pre-ART VLs available, and there was no significant difference between two groups (*SI Appendix*, Fig. S1*B*). $CD4^+$ T cell counts between two groups were not significantly different before and during ATI (Fig. 1*B*), and as expected, VLs were higher in NCs compared to PTCs at both the early and late post-ATI time points (Fig. 1 *A* and *C*). ART levels were undetectable during ATI in PTCs.

Human leukocyte antigen (HLA) typing information was available for 56 participants. PTCs and NCs demonstrated comparable distribution (Fisher's exact test, $P = 0.7$) of protective and susceptible HLA-B alleles (14) (*SI Appendix*, Fig. S1*C*).

Longitudinal Analysis of HIV Reservoir Size. In the Viro-Immunological Sustained CONtrol after Treatment Interruption (VISCONTI) study, one of the most detailed studies describing PTCs in early-treated PWH, HIV reservoir size measured by total cell-associated HIV DNA (CA-DNA) showed a tendency of declining in five of eight PTCs (12). However, this analysis was limited by small sample size and restricted to only early-treated PTCs and total HIV DNA levels. In order to characterize HIV reservoir size in a more comprehensive way, we evaluated multiple HIV reservoir-related markers longitudinally in this study. We performed an intact proviral DNA assay (IPDA) (15) in a subgroup of participants with available samples (PTC: n = 11, and NC: n = 13) since only intact proviruses have the potential to produce infective virions (16). During suppressive ART (pre-ATI), levels of intact, defective, and

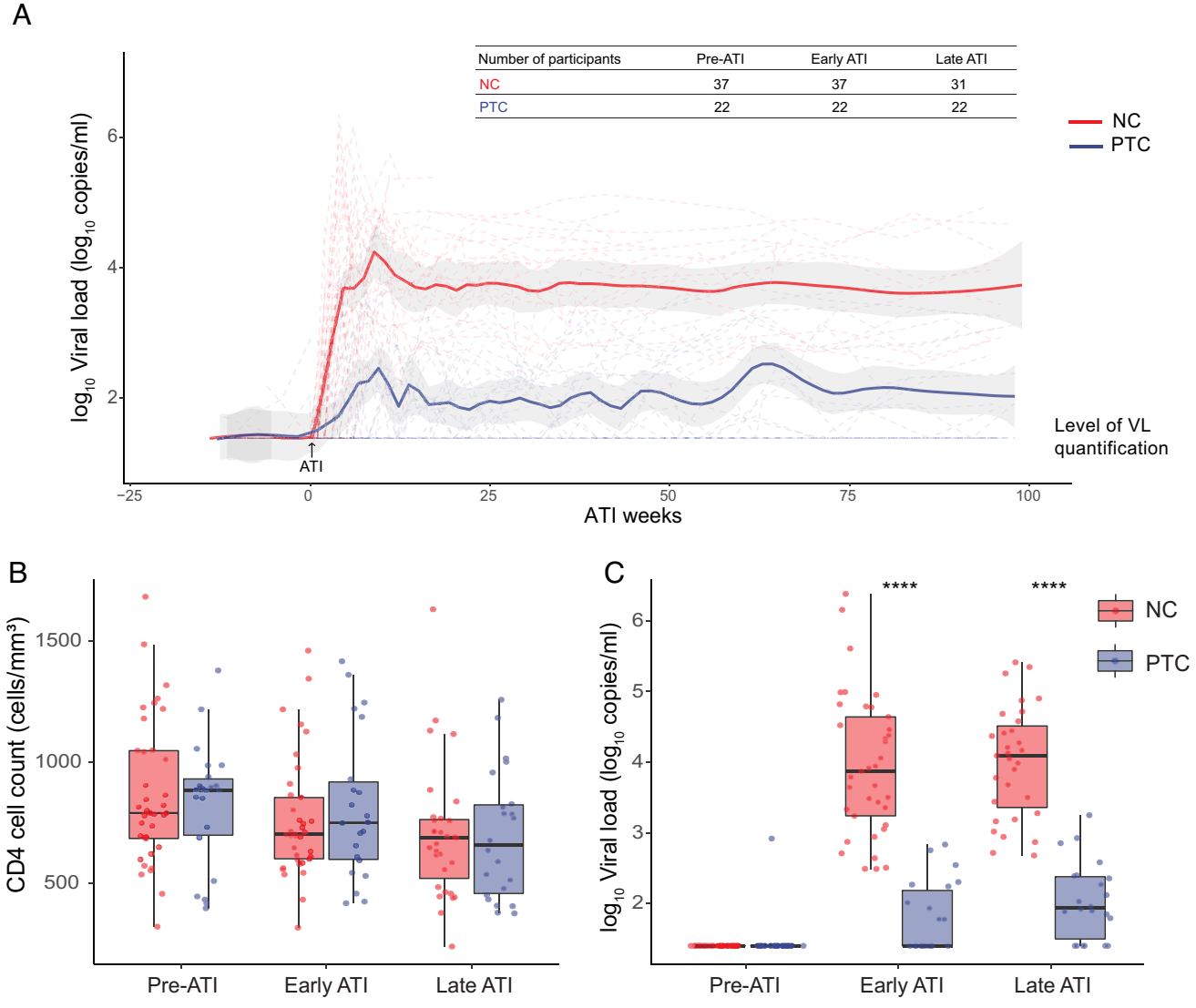

Fig. 1. Pre-ATI and ATI characteristics. (*A*) Viral load (VL) trajectory before and during ATI. Each participant's viral load trajectory is depicted in dotted lines in the background, and Loess curves with 95% (CI) are shown. (*B*) $CD4^+$ T cell count before and during ATI. (*C*) VL before and during ATI. Time point selection for PTCs and NCs is described in the Methods section. ****$P < 0.0001$.

total HIV DNAs were not significantly different between PTCs and NCs. However, during the ATI, intact, defective, and total HIV DNAs were significantly higher in NCs than in PTCs (Fig. 2 *A*–*C* and *SI Appendix*, Fig. S2*A*). There was no significant difference in the percentage of intact HIV DNA between PTCs and NCs either before or during the ATI (*SI Appendix*, Fig. S2*A*).

While on suppressive ART, there was no significant difference in the expression of the HIV reservoir as reflected by levels of

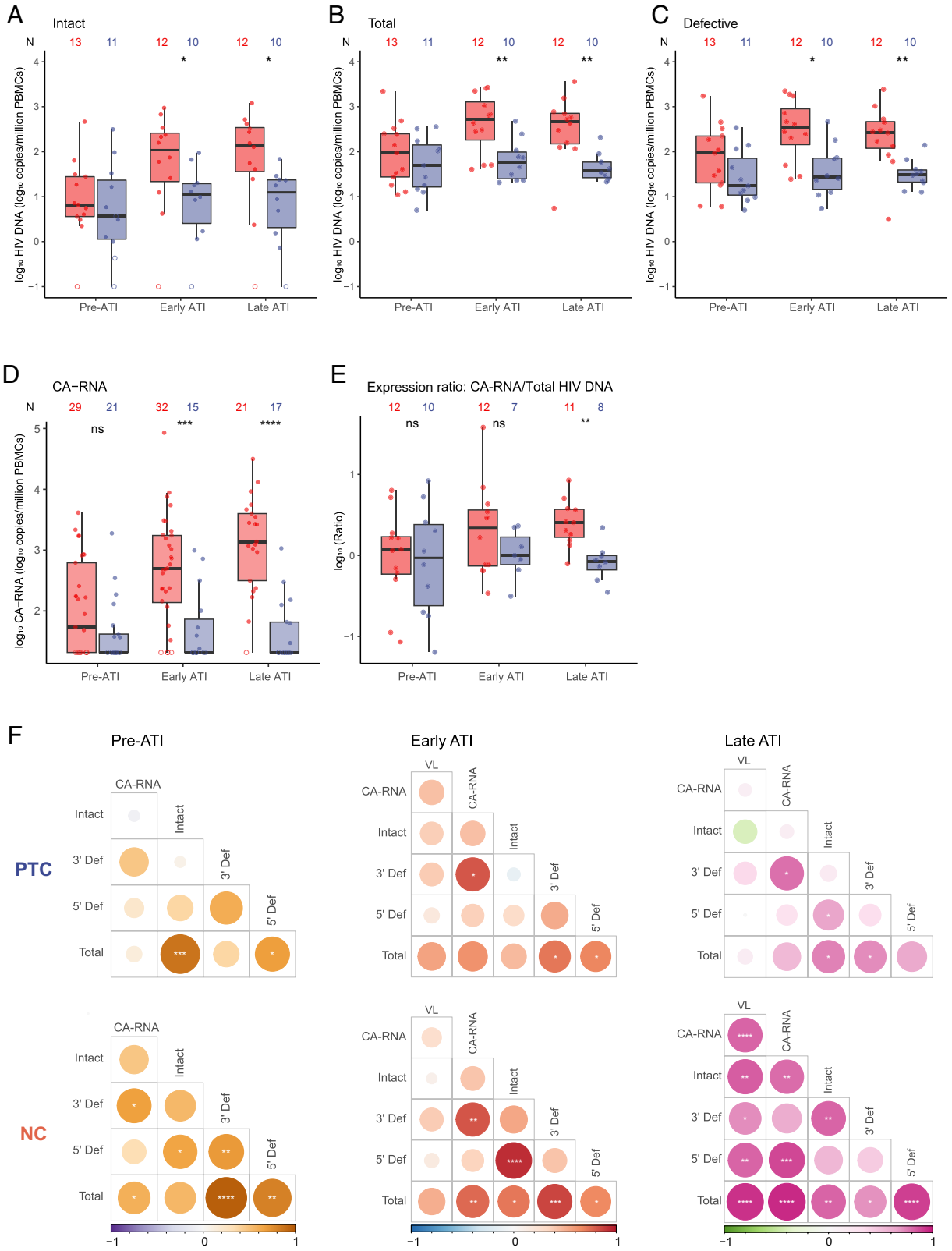

Fig. 2. Longitudinal analysis of HIV reservoir. Longitudinal (*A*) intact provirus from IPDA, (*B*) total provirus from IPDA, (*C*) defective provirus from IPDA, (*D*) CA-RNA, and (*E*) expression ratio (CA-RNA/total HIV DNA). Between-group comparison was conducted with the Wilcoxon rank-sum test adjusted for multiple time point comparisons with the Benjamini–Hochberg procedure. (*F*) Longitudinal Spearman correlation between different reservoir measurements. **P* < 0.05, ***P* < 0.01, ****P* < 0.001, and *****P* < 0.0001.

unspliced cell-associated RNA (CA-RNA) (Fig. 2*D*). During the ATI, PTCs maintained stable levels of CA-RNA at both the early and late time points. In contrast, NCs demonstrated rapid increases in CA-RNA during the ATI, with significantly higher levels compared to PTCs at both the early and late ATIs (Fig. 2*D*). We also evaluated longitudinal proviral transcriptional activity by evaluating the CA-RNA to total HIV DNA ratio (CA-RNA/total HIV DNA). After treatment interruption, NCs demonstrated a significantly higher CA-RNA/total HIV DNA expression ratio compared to the PTCs (Fig. 2*E*) that was concordant with dramatic increases in the HIV reservoir and plasma viral load after treatment interruption in NCs but not PTCs.

During the pre-ATI time period, CA-RNA was largely associated with levels of the 3′ defective HIV DNA (Fig. 2*F* and *SI Appendix*, Fig. S2*B*). This finding may be related to the enrichment of 3′ defective proviruses previously identified in central memory T cells and the relatively high levels of central and transitional memory T cells in the peripheral blood mononuclear cells (PBMCs) on suppressive ART (17). After treatment interruption, this relationship was maintained in the PTCs during both early and late ATIs. However, the differences in HIV reservoir activity were accentuated between PTCs and NCs during the late ATI period as intact and total HIV DNAs became highly correlated with rebound viral load and CA-RNA only in NCs but not PTCs (Fig. 2*F* and *SI Appendix*, Fig. S2*B*).

Longitudinal T Cell Composition, Immune Activation, and Exhaustion. Mounting evidence has shown that T cell composition, activation, and exhaustion significantly correlate with residual viremia on ART (18), tissue reservoir size (19), HIV persistence (19, 20), and ultimately, clinical outcomes (21–23). In the VISCONTI study, PTCs and ART-treated participants had a comparable level of $CD8^+$ T cell immune activation (CD38 and HLA-DR expression) (12), but the trajectory of T cell profiles during ATI remains uncertain. Thus, we investigated the dynamics of T cell composition, activation, and exhaustion in PTCs and NCs. A subgroup of participants (PTC: n = 10, and NC: n = 25) had T cell subsets and cellular inflammatory markers available for the pre-ATI and early ATI time points. Prior to ATI, PTCs and NCs had comparable $CD4^+$ T cell counts (median 886 vs. 814 cells/mm^3, $P > 0.9$). However, PTCs had a significantly higher CD4% (median 45.8% in PTCs vs. 34.4% in NCs, $P = 0.02$) and CD4/CD8 ratio (median 1.7 in PTCs vs. 1.1 in NCs, $P = 0.045$) (Fig. 3 *A*–*C*).

Due to the large number of features derived from multiparametric flow cytometry assays, we summarized the dynamic changes in a nonparametric normalized scale in Fig. 3*A*. T cells were categorized based on their expression of CD45RO levels into a mature/high functional group [total T cell (of the parent $CD3^+$ T cell count), central memory (T_{CM}), and effector memory T cells (T_{EM})], an immature/terminally differentiated/low functional group [naive (T_N), stem cell-like memory (T_{SCM}), and terminally differentiated effector memory T cells (T_{TDEM})]. Before ATI, differences in $CD4^+$ T cell-related phenotypes between PTCs and NCs were observed as PTCs had a higher CD4/CD8 ratio, higher mature/functional $CD4^+$ T cell%, higher nonfunctional $CD4^+$ T cell immune activation%, and lower functional mature/functional $CD4^+$ T cell exhaustion evaluated by PD-1 expression% (Fig. 3 *A*–*C*). During early ATI, both PTCs and NCs demonstrated increases in the levels of $CD8^+$ T cell activation, although only those from the NC group reached statistical significance (%$HLA–DR^+CD38^+$ in $CD8^+$ T cells in Fig. 3*C*). NCs had significant increases in activation levels in total $CD4^+$ T (pre-ATI vs. early ATI, median 0.96% vs. 1.25%, pairwise Wilcoxon signed-rank test, $P = 0.007$), $CD4^+$ T_{CM} (0.89% vs. 1.25%, pairwise signed-rank test, $P = 0.01$), and T_{EM} (1.47% vs. 2.40%, pairwise signed-rank test, $P = 0.03$), while PTCs maintained stable activation levels in these $CD4^+$ T cell subsets (global summary in Fig. 3*A* and %$HLA–DR^+CD38^+$ in $CD4^+$ T cells in Fig. 3*C*).

HIV reservoir measures did not show a significant correlation with specific T cell profiles before or during early ATI (*SI Appendix*, Fig. S3*A*). We observed a significant high-level correlation between PD-1 expression across different $CD8^+$ T cell subsets pre-ATI vs. early ATI (*SI Appendix*, Fig. S3*B*), suggesting a potential epigenetic imprinting at the exhaustion-related gene locus in $CD8^+$ T cells reported previously in HIV (24) and hepatitis C (25) infections.

Gag-Specific IFN-γ and IL-2 Secreting CD4+ T Cells Linked with Smaller HIV Reservoir Size. There is a complex interaction between HIV-specific T cells and the reservoir that shapes the landscape of HIV reservoir establishment, latency, and evolution (26–28). HIV-specific $CD4^+$ T cells are the preferential target for HIV infection (28) but are also associated with viral control during acute infection (27). In parallel, HIV-specific $CD8^+$ T cells play an important role in viral control (29, 30). It remains unknown how HIV-specific T cell dynamics affect or are affected by viral rebound and reservoir kinetics in PTCs and NCs. Pre-ATI, PTCs, and NCs had largely comparable levels of Gag-specific $CD4^+$ and $CD8^+$ T cells producing CD107a, IL-2, and MIP-1β (Fig. 4*A*). However, the level of Gag-specific TNF-α^+ $CD8^+$ T cells was significantly higher in NCs (Fig. 4 *A* and *B*). During early ATI, the Gag-specific $CD4^+$ IFN–γ^+ T cell levels became significantly higher in PTCs than in NCs, followed by a modestly higher level of $CD4^+$ IL-2^+ T cells (Fig. 4 *A* and *B*). Levels of polyfunctional HIV-specific $CD4^+$ and $CD8^+$ T cell responses were largely undetectable for both the PTCs and NCs. Pre-ATI, we observed a strong negative correlation between pre-ATI Gag-specific $CD4^+$ IFN–γ^+ T cells and CA-RNA (Fig. 4 *C* and *D*). None of the pre-ATI $CD8^+$ T cell markers correlated with HIV reservoir restriction/expansion (Fig. 4*C*). During the ATI, higher Gag-specific $CD4^+$ IFN–γ^+ and IL-2^+ T cell levels were also associated with lower rebound VL and CA-RNA (Fig. 4 *C* and *D*), suggesting their potential roles in restricting HIV reservoir expansion and viral rebound. In contrast, we did not observe a significant link between Gag-specific $CD8^+$ T cells with HIV rebound viral load (Fig. 4*C*).

Activated Functional NK Cells Correlated with HIV Reservoir Restriction. A growing body of evidence has suggested significant roles of natural killer (NK) cells in HIV control (31, 32). Hence, we next evaluated NK cell phenotype and functional dynamics during ATI. Globally, NK cell profiles between PTCs and NCs were similar (*SI Appendix*, Fig. S4), although PTCs tended to have a more activated CD56-negative ($CD56^-$) NK cell phenotype during early ATI compared to NCs (*SI Appendix*, Fig. S4, purple columns). PTCs had significantly higher levels of activation markers including %$CD38^+$ in $CD56^-$ NK pre-ATI and %$CD69^+$ in total NK (Fig. 5*A* and *SI Appendix*, Fig. S4). Certain NK function markers and %$CD38^+$ in total NK were negatively correlated with CA-RNA before ATI (Fig. 5 *B* and *C*). During early ATI, %$CD69^+$ in total NK and $CD56^{dim}$ NK became negatively correlated with rebound VL (Fig. 5 *B* and *C*). These results suggest a potential role of NK cell activation and function in restricting CA-RNA before ATI and suppressing viral rebound during early ATI.

Dynamics of Soluble Proinflammatory Markers during ATI. Several important soluble proinflammatory markers, including soluble CD14 (sCD14) and soluble CD163 (sCD163), are associated with morbidities and mortality in HIV infection (33). However, it remains largely unclear how they are associated with viral rebound during ATI. To this end, we evaluated the dynamics of certain

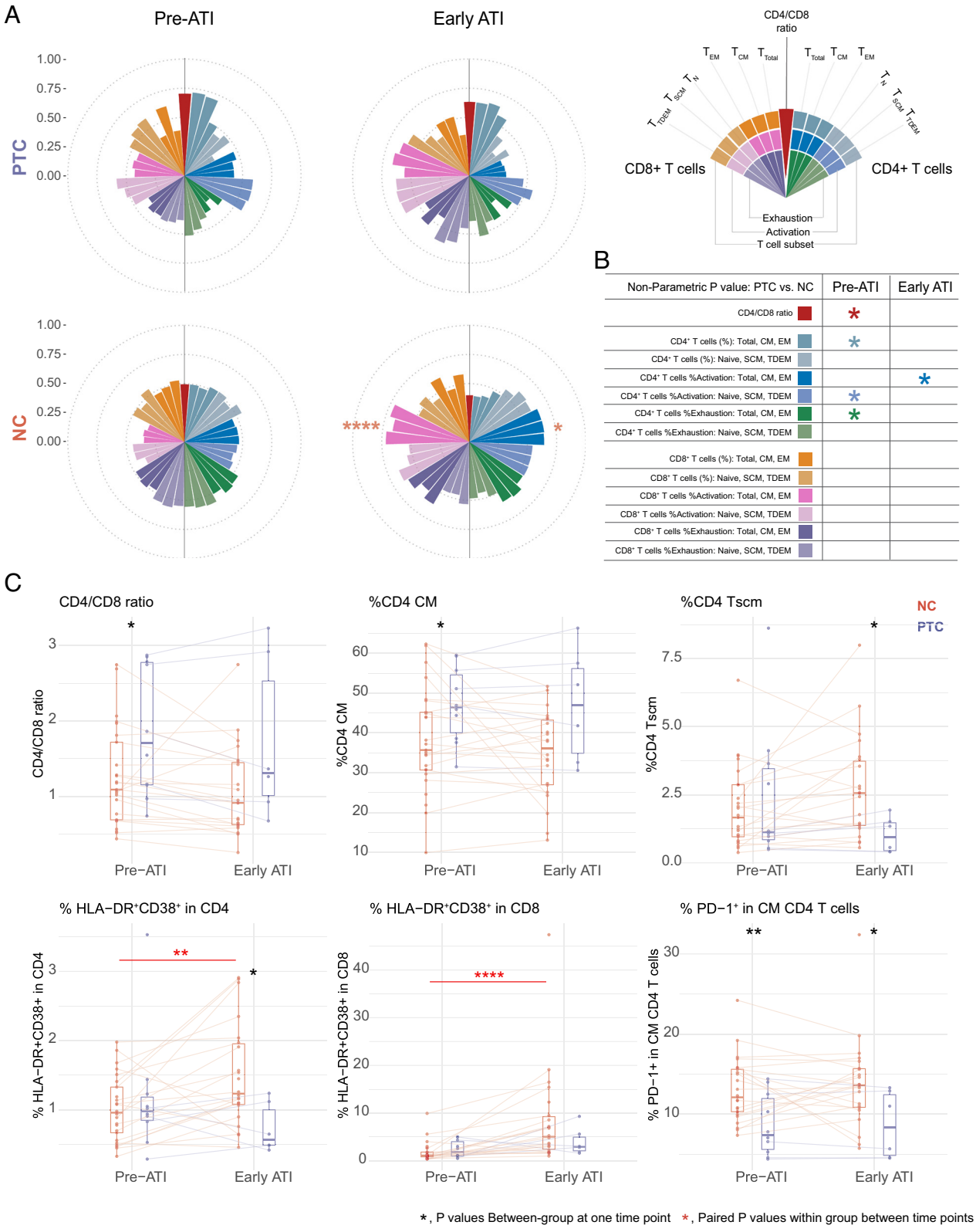

Fig. 3. Longitudinal trajectory in T cell subsets. (*A*) Polar plots describing global $CD4^+$ and $CD8^+$ T cell subset levels. The mean percentile level for each variable from each group at each time point is shown as the radius of the polar plot. Red asterisks indicate significant longitudinal changes in NCs by pairwise within-group comparisons. (*B*) Summary of between-group comparison in each T cell feature category. Adonis nonparametric MANOVA was used to compare between-group differences in each T cell feature category. (*C*) Selected T cell features with significant between-group differences or longitudinal differences. Black asterisks, between-group differences (Wilcoxon rank-sum test); red asterisks, within-group longitudinal differences (pairwise Wilcoxon signed-rank test). *$P < 0.05$, **$P < 0.01$, and ****$P < 0.0001$.

inflammatory markers in PTCs and NCs. Pre-ATI, there were no significant differences in any of the inflammatory markers between PTCs and NCs (Fig. 6*A*). During ATI, we observed significantly higher interleukin 10 (IL10) and interferon-γ (IFN-γ)–induced protein 10 (IP10) in NCs compared to PTCs. NCs also experienced a significant increase in the levels of IP10, sCD163, IFN-γ, and IL10

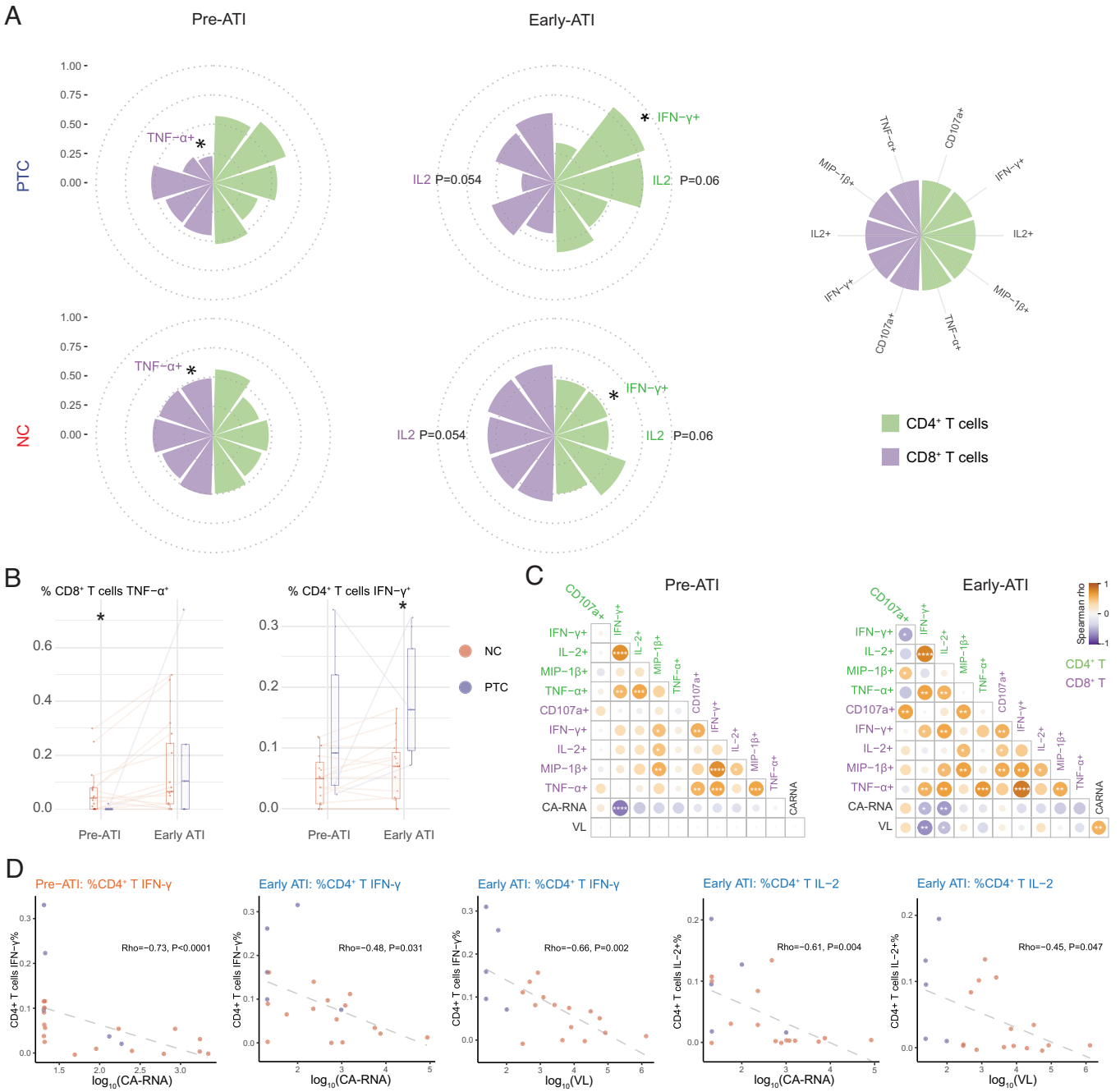

Fig. 4. T cell function and HIV viral control. (*A*) Polar plots describing global CD4$^+$ and CD8$^+$ T cell cytokine secretion upon Gag peptide pool stimulation. Mean percentiles are shown in the polar plot. (*B*) %CD8$^+$ T cells secreting TNF-α and %CD4$^+$ T cell secreting IFN-γ, the two T cell function features that were significantly different between PTCs and NCs. Medians (line) and individual data were shown for both PTCs and NCs. (*C*) Pairwise Spearman correlation between CD4$^+$, CD8$^+$ T cell function, and HIV virology parameters. (*D*) Selected correlation plots between T cell function and HIV virology parameters. Spearman correlation coefficient (Rho) and P values are shown. *P < 0.05, **P < 0.01, ***P < 0.001, and ****P < 0.0001.

during the ATI (Fig. 6*A*). Overall, there were stronger correlations between reservoir size and inflammatory markers in NCs than in PTCs, especially during early ATI (Fig. 6*B*). This finding suggests that pronounced VL rebound and HIV reservoir expansion in the early ATI period are tightly linked with a hyperinflammatory environment in NCs but not PTCs.

Viro-immunological Network Associated with Post-treatment Control

In order to define a minimal set of the most important pre-ATI viro-immunological features associated with post-treatment control, we used the sparse partial least squares discriminant analysis (sPLS-DA) (34) to evaluate a subgroup of 28 participants (PTC: n = 8, and NC: n = 20) with complete pre-ATI viro-immunological data (including CA-RNA, cytokines, T cell subsets, and NK subsets/function; due to missing data, IPDA and T cell functional profiles were not included). Fourteen features were selected from the pre-ATI time point, which were able to clearly separate PTCs from NCs (Fig. 7*A*). The major contributing factors (contribution >5%) for Component 1 highlighted an enrichment of elevated pre-ATI %CD4, CD4/CD8 ratio, CD56$^-$ NK activation in PTCs, along with low levels of CD4$^+$ T cell senescence (%CD4$^+$ T_{TDEM}), CD4$^+$ T cell exhaustion, and CA-RNA (Fig. 7*B*). These factors had an excellent accuracy to distinguish PTCs from NCs pre-ATI

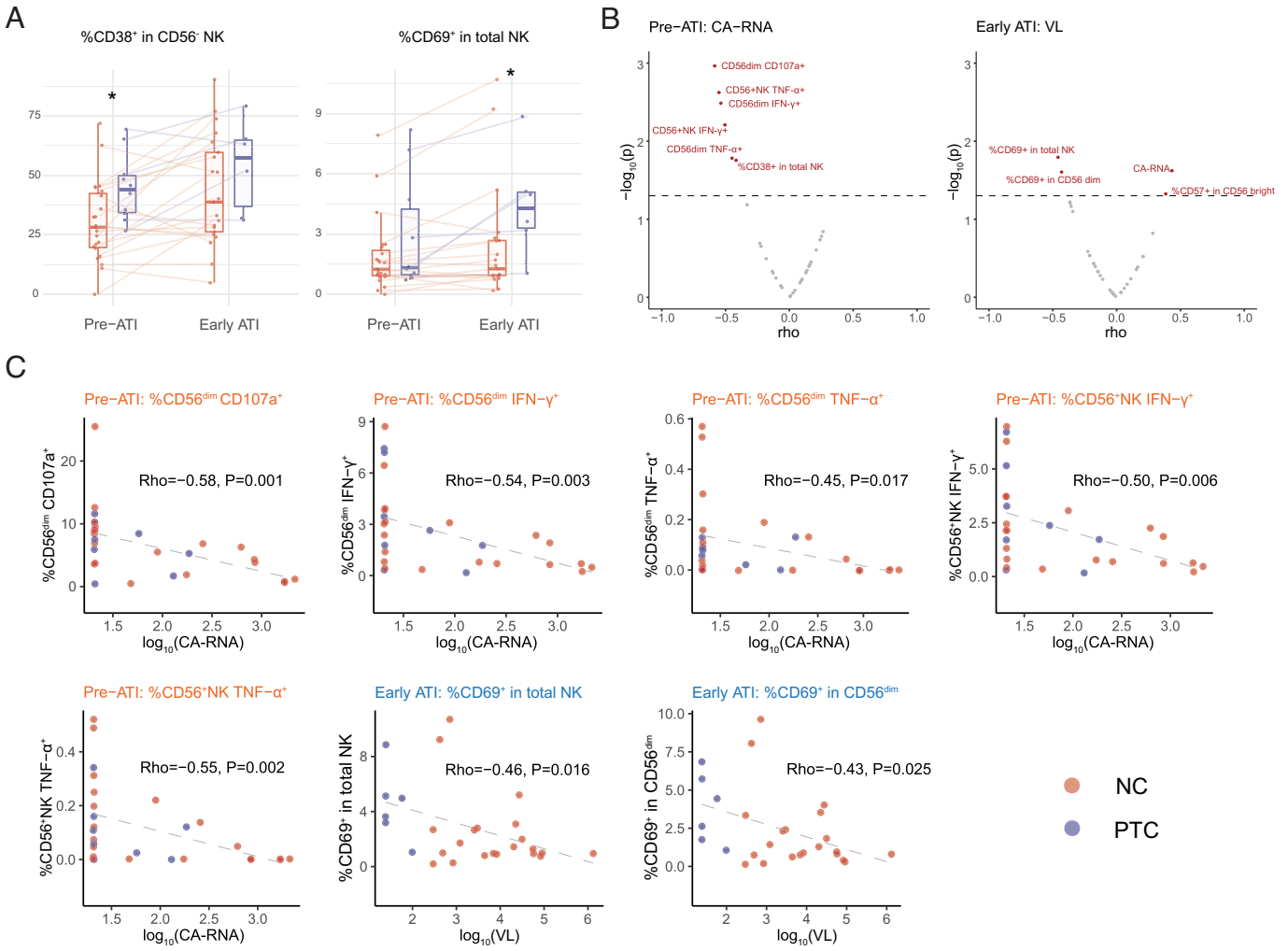

Fig. 5. NK cell phenotype and function. (*A*) %CD38$^+$ in CD56$^-$ NK cells and %CD69$^+$ in total NK cells, two NK activation markers that were significantly different between PTCs and NCs. (*B*) Correlation plots between NK features and CA-RNA before ATI and VL in early ATI. (*C*) Correlation plots demonstrating a significant correlation between NK features and virological features pre-ATI and early ATI. Spearman correlation coefficient (Rho) and *P* values are shown. *$P < 0.05$, **$P < 0.01$, ***$P < 0.001$, and ****$P < 0.0001$.

(area under the curve of ROC, 0.91) (Fig. 7*C*). Altogether, factors selected by sPLS-DA were highly correlated with other immunological features in this dataset (Fig. 7*D*). Notably, unsupervised clustering using selected features was able to distinguish most PTCs from NCs; however, PTCs demonstrated a heterogeneous enrichment in these favorable features, with overall low levels of unfavorable features (Fig. 7*E*).

Similarly, we conducted sPLS-DA to explore viro-immunological features during early ATI (PTC: n = 6, and NC: n = 22). Seventeen features were selected from the early ATI dataset that distinguished PTCs from NCs (*SI Appendix*, Fig. S5*A*). The major contributing factors (contribution >5%) again highlighted an enrichment in high levels of %CD4, CD4/CD8 ratio, %CD4$^+$ T_{CM}, and exhaustion of CD4$^+$ T_{SCM} (*SI Appendix*, Fig. S5*B*). In contrast, high levels of CD4$^+$ T cell activation (HLA-DR$^+$ and CD38$^+$ in total CD4$^+$ T, T_{CM}, and T_{EM}), T cell exhaustion (PD1$^+$ in CD4$^+$ T_{CM} and CD8$^+$ T_{EM}), immature T cells (CD4$^+$ T_{SCM}), and inflammation (IP10) in early ATI were enriched in NCs (*SI Appendix*, Fig. S5*B*).

Discussion

In this study, we performed longitudinal virological and immunological profiling to identify important features accounting for post-treatment control. We show that PTCs are capable of controlling their HIV reservoir expansion and expression during ATI along with plasma viral load control. This control over reservoir expansion and rebound is further tied to a lower level of proinflammatory markers, lower levels of activation in mature/functional CD4$^+$ T cell groups, and more robust HIV Gag-specific CD4$^+$ T activity, NK cell activation, and function. Furthermore, we defined a set of pre-ATI virological and immunological markers that differentiated PTCs from NCs.

Elevated levels of HIV DNA and CA-RNA have been associated with earlier timing of viral rebound in previous studies (6, 35, 36). In our study, detectable levels of pre-ATI proviral DNA and CA-RNA could be found in both PTCs and NCs and did not preclude the possibility of post-treatment control. In general, HIV reservoir size was more limited in PTCs and in the multivariable analysis; lower levels of pre-ATI CA-RNA contributed to the ability to differentiate PTCs from NCs. In addition, a number of PTCs were found to have transient periods of detectable viremia during ATI but no evidence of reservoir expansion or increased cellular viral RNA expression. There was also little fluctuation in T cell subset proportions in the PTCs, with largely stable levels of CD45RO$^+$ T cell population (mostly T_{CM} and T_{EM}) and CD45RO$^-$T cell population (mostly T_N and T_{SCM}). Together, these findings suggest that an efficient antiviral immune response may mediate the virological control by limiting the expansion and

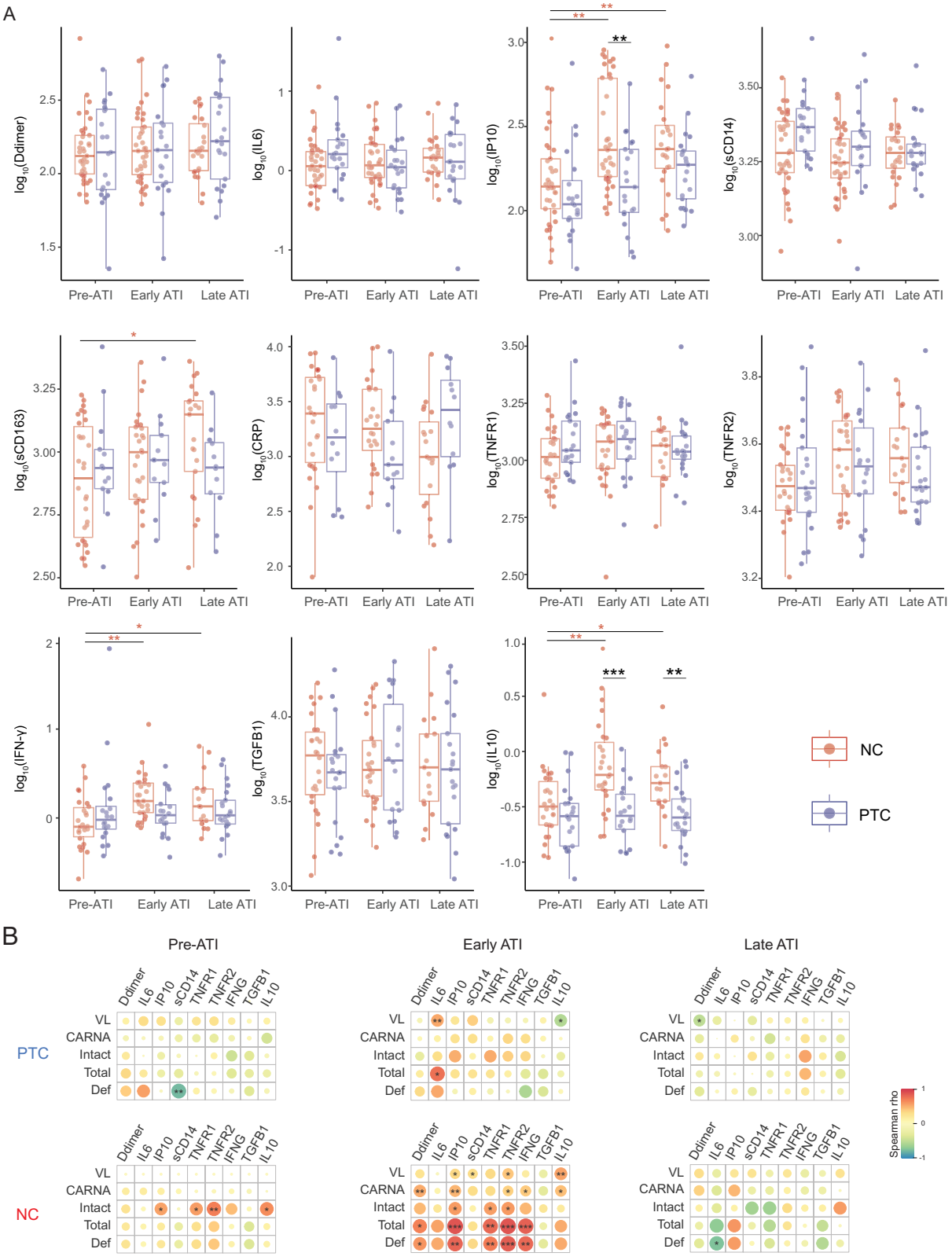

Fig. 6. Longitudinal analysis of soluble proinflammatory markers. (*A*) Dot and Tukey box plots describing the longitudinal trajectory of soluble proinflammatory markers. Black asterisks indicate between-group comparison at one time point, adjusted for multiple comparisons with the Benjamini–Hochberg procedure. Red asterisks indicate significant longitudinal changes in NCs by pairwise within-group comparisons. For D-dimer, IL6, IP10, and sCsD14, 37 NCs and 21 PTCs had results available before ATI. For sCD163, 30 NCs and 13 PTCs had result available before ATI. For TNFR1, TNFR2, IFN-γ, TGFβ1, and IL10, 26 NCs and 20 or 21 PTCs had pre-ATI results available. For CRP, 26 NCs and 12 PTCs had pre-ATI results available. (*B*) Exploratory analysis assessing correlation between reservoir measures and proinflammatory markers. Pairwise Spearman correlation analysis was performed for each group at each time point. *$P < 0.05$, **$P < 0.01$, ***$P < 0.001$, and ****$P < 0.0001$.

transcription of the viral reservoir. The marked differences in HIV reservoir size and activity at the late post-ATI time point are especially notable given that PTCs were sampled a median of 96 wk after ATI, while NCs were sampled a median 16 wk after ATI. Our findings on reservoir dynamics are consistent with the VISCONTI study (12) and a recent report on two PTCs from

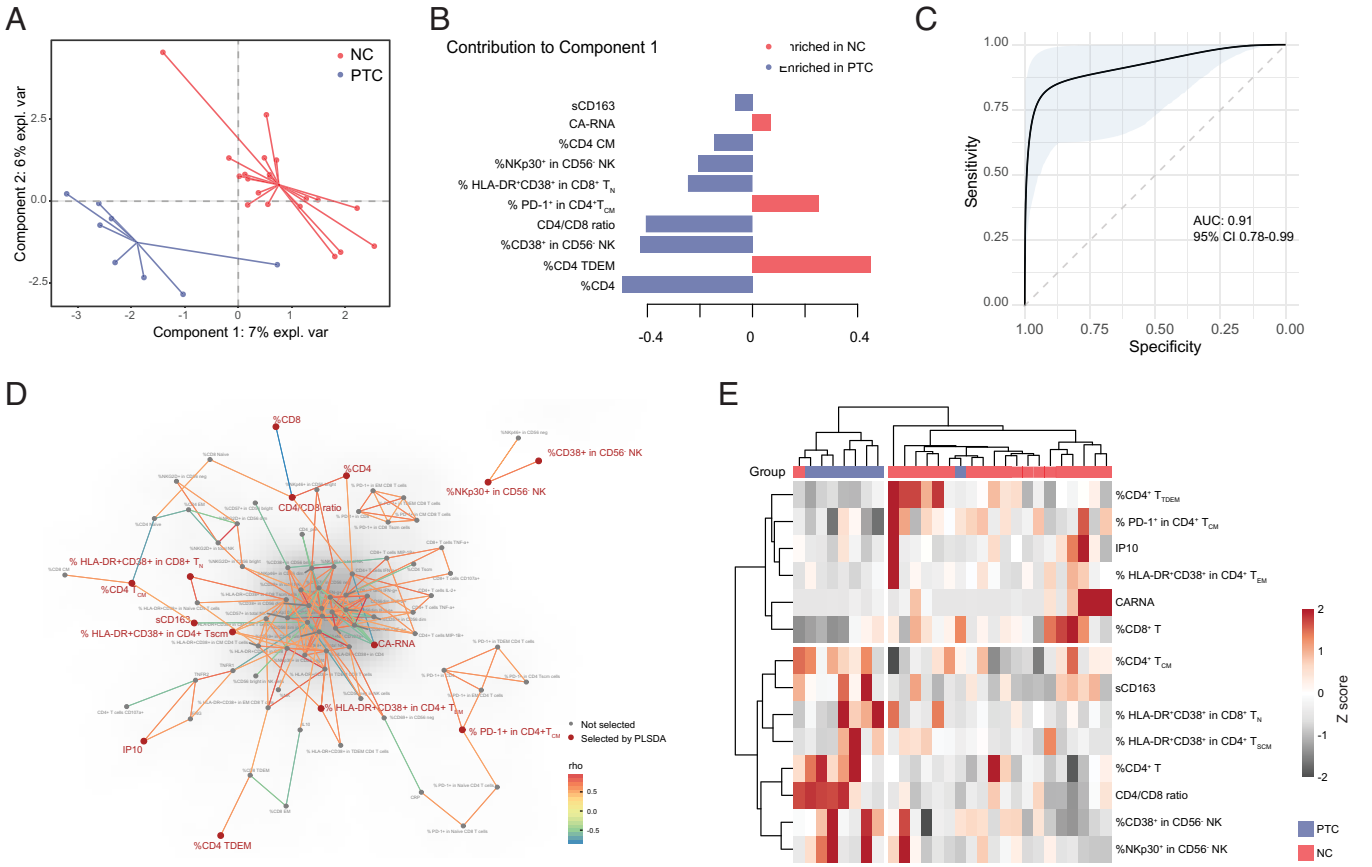

Fig. 7. Viro-immunological features associated with post-treatment control. (*A*) PLS-DA plot after feature selection. (*B*) Features contributing to Component 1, with a contribution rate >0.05, are plotted. (*C*) Receiver operating characteristic curve for Component 1. (*D*) Correlation network plot highlighting selected features. Pairwise Spearman correlations are calculated, and only those with Spearman coefficient Rho absolute values > 0.5 and $P < 0.01$ are included. (*E*) Heat map including selected features. Ward's hierarchical clustering was performed. Each feature is scaled to Z score.

Blazkova and Gao et al. (37), who also report stable HIV reservoir size during treatment interruption in PTCs. Differences in HIV transcription between HIV PTCs and NCs were also recently reported using a droplet digital PCR platform that measured levels of initiated, 5′-elongated, midelongated, completed, and multiply spliced HIV transcripts (38). The results showed that after treatment interruption, there was no significant increase in HIV transcriptional initiation in either PTCs or NCs. Instead, the primary differences were in the dramatic increases in multiply spliced and completed transcripts in NCs that were not seen in PTCs. Together, these studies highlight the ability of PTCs to limit viral transcription as a distinguishing feature for HIV post-treatment control.

PTCs demonstrate a unique set of immunological profiles compared to NCs, highlighting their capability of maintaining lower inflammation and T cell activation (especially in $CD4^+$ T cells) along with reservoir restriction. This could potentially play a role in the reduced susceptibility to viral replication as activated $CD4^+$ T cells have been linked to a higher level of HIV proviral transcription (39), susceptibility to new infection (40), and HIV viral persistence (41). This finding is also in stark contrast with HIV elite controllers (EC) and viremic controllers, who have been found to have significantly higher levels of T cell activation than those on ART (2, 12, 42, 43). In addition, ECs have also been found to have elevated levels of several soluble inflammatory markers despite maintaining viral control, suggesting that ECs maintain viral control at a cost of systemic inflammation (44). In comparison, PTCs demonstrate a lower level of soluble proinflammatory markers during ATI, especially IP10 and IL10. We also demonstrate a lack of correlation between viral reservoir expansion and proinflammatory markers in PTCs when compared to NCs. The elevated IP10 levels in NCs are likely related at least in part to increased resumption of viral replication as previous reports showed that participants of the Strategies for Management of Antiretroviral Therapy study who were randomized to the drug conservation arm were also found to have higher IP10 levels (45), and IP10 levels have been associated with elevated viremia in other studies (46, 47). In contrast to PTCs, NCs were found to have increasing sCD163 levels post-ATI associated with rebounding viremia and is consistent with a small study of participants treated during primary infection who underwent an ATI (48). sCD163 is a marker of monocyte/macrophage activation and has been associated with the development of noncalcified coronary plaques in both chronic-treated PWH and HIV ECs (49–51). In conjunction with the elevated markers of T cell activation, these results highlight the rapid reactivation of both the innate and adaptive immune system in response to viral rebound and underscore the risks of long-term treatment interruption in NCs (52). In comparison, PTCs showed no significant increases in either T cell activation or soluble markers of monocyte/macrophage activation. These intriguing results are likely due to the low levels of viral replication seen in the PTCs and suggest that PTCs could be at lower risk of adverse clinical outcomes compared to either NCs who undergo treatment interruption or potentially HIV ECs.

In defining potential mechanisms of HIV post-treatment control, we identified both T cell and NK cell functional activity that could be playing a role in limiting the size of the HIV reservoir and suppressing viral rebound. We evaluated levels of Gag-specific

T cell activity and found a higher level of HIV-specific $CD4^+$ cells expressing IFN-γ and IL-2 in PTCs compared to NCs. These markers were significantly associated with a restricted reservoir size and lower viral rebound during early ATI. Immune profiling of HIV elite controllers has shown an enrichment in protective HLA alleles and polyfunctional HIV-specific CD8 T cell responses that point to this as a vital immune mediator of natural HIV control (5, 53). In contrast, Gag-specific $CD8^+$ T cells did not seem to contribute to post-treatment control or reservoir restriction, which suggests that PTCs are able to achieve HIV remission through alternative immune pathways. The association of HIV-specific IFN-γ^+ $CD4^+$ T cell activity with viral kinetics after treatment interruption is consistent with the results of the ACTG trial A5197, a study of an Ad5 HIV *gag* therapeutic vaccine. In that trial, levels of HIV-specific $CD4^+$ cells expressing IFN-γ were inversely associated with viral load set point (54).

In addition to Gag-specific $CD4^+$ T cells, we also demonstrated several NK cell features that were associated with post-treatment control and a lower level of HIV CA-RNA and rebound viral load. NK cells play a significant role in restricting HIV replication during untreated infection (55). Emerging evidence has suggested that NK cells, especially mature subpopulations (56) including $CD56^-$ and $CD56^{dim}$ (57) NK cell activation and function, are associated with early ART initiation in PWH and viral control in ECs (58). In a humanized-mice model study, Kim et al. demonstrated that adoptive NK cell infusion into humanized, HIV-infected, virally suppressed mice delayed viral rebound during ATI and decreased the tissue reservoir diversity (32). In a pediatric HIV cohort, an HLA-I signature favoring killer cell immunoglobulin-like receptor (KIR) education and subsequent NK cell function was also linked to slower disease progression (59). In addition, antibody-mediated NK cell activation was recently found to be associated with delayed viral rebound in an ATI cohort study (60). Furthermore, the VISCONTI study has also demonstrated an important role of NK cell function in controlling HIV infection (61). These findings in sum have pointed to an important role in HIV restriction by NK cells across different clinical phenotypes in HIV infection. Further deep immunophenotyping of NK cells KIR typing would be warranted to further reveal the underlying mechanisms between HIV control and NK cell phenotype/function.

This study has a few limitations. First, due to sample availability, only a subgroup of participants had IPDA, soluble proinflammatory markers, and flow cytometry data available. Participants with suppressed viral load tested by a standard clinical assay rather than a single-copy assay, which precluded us from detecting a difference in very low-level viremia between PTC and NC groups. Second, all participants were enrolled >15 y ago while they were suppressed on older ART regimens, although the ACTG study A5345 demonstrated that viral rebound kinetics for NCs did not differ in those receiving newer ART regimens (7). Third, further work needs to be done to evaluate the role of intact proviral integration sites in defining post-treatment control, especially as proviral integration into areas of deep latency has been described in ECs (62, 63) and PWH receiving long-term ART (64). Given limited PBMC availability for cell function assays, Pol- and Nef-specific T cell functions were not able to be evaluated. Finally, we did not evaluate the contribution of humoral immunity in post-treatment control. It is likely that HIV post-treatment control is a multifactorial process, and humoral immunity may play a key role in those with less robust NK and/or T cell activity. As shown in a recent study, two PTCs with >200-wk follow-up demonstrated distinct mechanisms for maintaining post-treatment viral control (37). One participant demonstrated stronger T cell response, while the other showed strong autologous neutralizing antibody activity that was postulated to have mediated viral control (37). Further studies are underway to evaluate humoral immunity and post-treatment control.

In summary, PTCs serve as a natural model for sustained HIV remission and thus represent a crucial population for future HIV cure research. Our study expands the understanding of post-treatment control, and the set of distinguishing viro-immunological features of PTCs may help identify those likely to achieve HIV post-treatment control prior to an ATI and could be factored into the design of future ATI trials. In addition, our results suggest that therapeutic strategies boosting both HIV-directed $CD4^+$ T cells and NK cells may be required to achieve ART-free HIV remission.

Materials and Methods

Study Population and Time Points. We included PTC and NC participants who were originally identified in the CHAMP study (13) from prior AIDS Clinical Trials Group (ACTG) analytical treatment interruption (ATI) studies (54, 65–71). PTCs maintained viral loads ≤400 HIV RNA copies/mL at ≥2/3 of time points for ≥24 wk after the ATI. NCs were identified among those in the same study arm who did not meet the PTC criteria and had available stored samples. Viro-immunological profiling was conducted prior to ATI and during ATI (early and late). For this study, we planned on evaluating viro-immunological responses during early and late ATI courses. Due to a more rapid and pronounced viral rebound in NCs, ART was resumed earlier in this group, and they in general had a shorter ATI duration (*SI Appendix*, Fig. S6). Early post-ATI viro-immunological profiling was performed a median of 4 wk post-ATI for NCs vs. 12 wk for PTCs, and the median post-ATI weeks for the late ATI profiling were 16 and 96, respectively. The slightly delayed early post-ATI sampling for the PTCs was to assess the viro-immunological phenotype in PTCs after any transient early post-ATI viral rebound, which was seen in a subset of PTCs prior to viral control and described in the original description of the CHAMP study (13).

Study Approval. Participant samples were collected according to protocols approved by the Mass General Brigham Institutional Review Board. This current study protocol was approved by Mass General Brigham Institutional Review Board with the protocol #2014P000661/BWH. Participants provided a written informed consent in accordance with the Declaration of Helsinki.

HIV Reservoir Quantification. CA-RNA was isolated from cryopreserved peripheral blood mononuclear cells (PBMCs) using the AllPrep DNA/RNA Mini Kit (Qiagen). Unspliced CA-RNA level was quantified using a real-time PCR approach with primers/probes targeting conserved regions of HIV LTR/gag as previously described (6, 72). Cell numbers were quantified by the real-time PCR measurement of CCR5 copy numbers. Cellular integrity for RNA analysis was assessed by the measurement of total extracted RNA and evaluation of the IPO8 housekeeping gene (73). CA-RNA levels below the limit of quantification (20.73 copies/million PBMCs) were categorized as below quantification/detection range and assigned the values of 20.73 RNA copies/million PBMCs for analysis.

Intact Proviral DNA Assay (IPDA). IPDA was performed at AccelevirDx per the protocol published in their previous study (15).

HLA Typing. HLA class I typing was performed following the PCR-SSOP (sequence-specific oligonucleotide probing) and the PCR-SBT (sequence-based typing) protocols recommended by the 13th International Histocompatibility Workshop. We included protective and susceptible HLA-B alleles based on previous reports (14, 74) (*SI Appendix*, Table S3). Concurrent protective and susceptible alleles were counted as neutral alleles.

Soluble Markers of Inflammation. Soluble markers of inflammation were measured with ELISA-based assays. Plasma was analyzed for levels of IL-6, sCD14, IP10, sCD163, CRP, TNFR1 and TNFR2 (all from R&D Systems, Minneapolis, MN), D-dimer (Diagnostica Stago, Parsippany, NJ), and IL10 and TGFβ (both from MSD, Rockville, MD) per the manufacturers' protocols. Since these markers were measured in two batches, we examined the batch effect of the overlapping tests and did not find batch effect (*SI Appendix*, Fig. S7).

Immune Phenotyping and Intracellular Cytokine Staining (ICS). Approximately 10^6 PBMCs were used for T and NK cell phenotyping. T cells were stained with blue viability dye (Invitrogen) and for chemokine receptor CCR7 at 37 °C for 20 min and then followed by a master mixture of antibodies targeting CD3, CD8, CD4, CD45RO, CD95, HLA-DR, CD38, and PD-1 at 4 °C for 20 min. NK cells were stained with blue viability dye and antibodies targeting CD3, CD19, CD16, CD56, CD69, CD38, CD57, NKG2D, NKp30, and NKp46 (*SI Appendix, Method*).

T cell intracellular cytokine staining (ICS) was performed on PBMCs stimulated with a HIV Gag peptide pool, and NK cell ICS was performed with PBMCs stimulated with K562 cells. For T cells, approximately 10^6 cells were stimulated overnight with anti-CD28/49d (0.5 μg/mL; BD) and 2 μg/mL synthetic peptides (overlapping 15- to 20-mer Gag peptide pools spanning the entire clade B consensus sequence of the HIV-1 *gag* sequence). NK cells were stimulated overnight with K562 cells with an effector-to-target ratio of 10:1, and brefeldin A (1 μg/mL; BioLegend), Monensin Solution (1 μg/mL; BioLegend), and CD107a antibody were added after 1-h culture and incubated for an additional 5 h. Cells stimulated with PMA (2.5 μg/mL) and ionomycin (0.5 μg/mL) served as a positive control, and R10 medium only served as a negative control. After stimulation, the cells were stained with surface antibodies against CD3, CD19, CD16, CD56, and blue viability dye at 4 °C for 20 min. Subsequently, cells were treated with a fixation and permeabilization solution according to the manufacturer's protocol. Cells were stained for 20 min at room temperature with antibodies directed to IFN-γ, IL-2, CD107a, and TNF-α. Cells were then fixed by 2% PFA (Affymetrix), acquired on an LSRFortessa flow cytometer (BD), and analyzed using FlowJo (version v10) software (Tree Star). The proportion of cytokine-secreting cells had to be greater than 0.1% after subtraction to be considered a positive response.

Measurements of Antiretroviral Drug Concentrations. Plasma concentrations of nevirapine (NVP), abacavir (ABC), and lamivudine (3TC) were measured by a validated high-performance liquid chromatography method as previously described (75). ARV drug concentrations were compared to previously described steady-state pharmacokinetics for NVP (76), ABC (77), and 3TC (78). All assay methods have been validated internally and through external proficiency testing by the DAIDS Clinical Pharmacology Quality Assurance and Quality Control Program.

Statistical Analysis. We used the Wilcoxon rank-sum test to evaluate between-group differences. *P* values for multiple comparisons involving >2 time points between PTCs and NCs were corrected with the Benjamini–Hochberg method. A within-group comparison between different time points was conducted with either the paired Wilcoxon signed-rank test if there were only two time points or Dunn's test with Benjamini–Hochberg adjustment if there were three time points. Categorical variables were compared using either the chi-squared test or Fisher's exact test. Correlations between HIV reservoir, viral load, and inflammatory and immune markers were determined with the Spearman test. Statistical analyses were performed with R (4.1.0) and Stata (13.0, College Station, TX), and figures were plotted with the R "ggplot2" package unless otherwise specified. Details in statistical models, including polar plot generation, PLS-DA, were included in the *SI Appendix, Method* section.

Data, Materials, and Software Availability All study data are included in the article and/or *SI Appendix*. Some study data available (Data are available upon request to the AIDS Clinical Trials Group by submitting a Data Request form: https://submit.mis.s-3.net/).

ACKNOWLEDGMENTS. We thank the participants, staff, and investigators of the ACTG studies A371 (Paul Volberding and Elizabeth Connick), A5024 (J. Michael Kilby and R.M.), A5068 (J.M.J., I.F., M.S., and J.J.E.), A5170 (D.S., D.M.M., and D.H.), and A5197 (R.T.S., M.M.L., and D.H.). We appreciate Michael Bale's help with the panmixia testing, Laura Gray's assistance with single genome sequencing (SGS), and the help of Nicole Stange-Thomann and the Massachusetts General Hospital Center for Computational and Integrative Biology DNA Core. This study was funded in part by the American Foundation for AIDS Research and NIH grants AI068634, AI068636, AI106701, AI150396, AI164560, P30 AI045008, UM1 AI069534, and AI069412. Y.L. was funded by NIH T32 training grant (5T32AI007387-32, PI Kuritzkes, Daniel). R.T.G. and J.Z.L. received grant funding from the Harvard University Center for AIDS Research (NIH P30 AI060354). This project has also been funded in whole or in part with federal funds from the Frederick National Laboratory for Cancer Research, under Contract No. HHSN261200800001E. This research was supported in part by the Intramural Research Program of the NIH, Frederick National Lab, Center for Cancer Research.

Author affiliations: [a]Department of Medicine, Brigham and Women's Hospital, Harvard Medical School, Boston, MA 02139; [b]Ragon Institute of Massachusetts General Hospital, Massachusetts Institute of Technology, and Harvard, Cambridge, MA 02139; [c]School of Medicine, Case Western Reserve University, Cleveland, OH 44106; [d]Harvard T. H. Chan School of Public Health, Boston, MA 02115; [e]School of Medicine, University of Alabama at Birmingham, Birmingham, AL 35233; [f]Basic Science Program, Frederick National Laboratory for Cancer Research, National Cancer Institute, Frederick, MD 21702; [g]Laboratory of Integrative Cancer Immunology, Center for Cancer Research, National Cancer Institute, Bethesda, MD 20814; [h]Department of Medicine, Massachusetts General Hospital, Harvard Medical School, Boston, MA 02114; [i]School of Medicine, University of California San Francisco, San Francisco, CA 94143; [j]Department of Medicine, University of Arizona, Tucson, AZ 85724; [k]School of Medicine, University of California Los Angeles, Los Angeles, CA 90095; [l]School of Medicine, University of Pennsylvania, Philadelphia, PA 19104; [m]Department of Medicine, University of North Carolina at Chapel Hill, Chapel Hill, NC 27599; [n]Department of Medicine, University of Massachusetts Chan Medical School - Baystate, Springfield, MA 01199; and [o]Department of Medicine, University of California San Diego, San Diego, CA 92103

Author contributions: B.E., X.S., R.G., J.M.J., P.V., E.C., R.M., I.F., M.S., J.J.E., D.S., D.M.M., D.H., R.T.S., M.M.L., and J.Z.L. designed research; B.E., X.S., Y.L., M.M., D.M., R.T.G., H.A., E.P.A., Y.Y., M.P.M., M.C., M.M.L., X.G.Y., and J.Z.L. performed research; B.E., X.S., Y.L., E.A., R.J.B., and J.Z.L. analyzed data; and B.E., Y.L., and J.Z.L. wrote the paper.

1. M. M. Lederman *et al.*, A cure for HIV infection: "Not in my lifetime" or "just around the corner"? *Pathog. Immun.* **1**, 154–164 (2016).
2. Y. Li, A. Mohammadi, J. Z. Li, challenges and promise of human immunodeficiency virus remission. *J. Infect. Dis.* **223**, S4–S12 (2021).
3. G. Hutter *et al.*, Long-term control of HIV by CCR5 Delta32/Delta32 stem-cell transplantation. *N. Engl. J. Med.* **360**, 692–698 (2009).
4. T. J. Henrich *et al.*, Long-term reduction in peripheral blood HIV type 1 reservoirs following reduced-intensity conditioning allogeneic stem cell transplantation. *J. Infect. Dis.* **207**, 1694–1702 (2013).
5. F. Pereyra *et al.*, The major genetic determinants of HIV-1 control affect HLA class I peptide presentation. *Science* **330**, 1551–1557 (2010).
6. J. Z. Li *et al.*, The size of the expressed HIV reservoir predicts timing of viral rebound after treatment interruption. *AIDS* **30**, 343–353 (2016).
7. J. Z. Li *et al.*, Time to viral rebound after interruption of modern antiretroviral therapies. *Clin. Infect. Dis.* **74**, 865–870 (2022).
8. M. C. Sneller *et al.*, Kinetics of plasma HIV rebound in the Era of modern antiretroviral therapy. *J. Infect. Dis.* **222**, 1655–1659 (2020).
9. C. Goujard *et al.*, HIV-1 control after transient antiretroviral treatment initiated in primary infection: Role of patient characteristics and effect of therapy. *Antivir. Ther.* **17**, 1001–1009 (2012).
10. S. Lodi *et al.*, Immunovirologic control 24 months after interruption of antiretroviral therapy initiated close to HIV seroconversion. *Arch. Intern. Med.* **172**, 1252–1255 (2012).
11. J. Maenza *et al.*, How often does treatment of primary HIV lead to post-treatment control? *Antivir. Ther.* **20**, 855–863 (2015).
12. A. Saez-Cirion *et al.*, Post-treatment HIV-1 controllers with a long-term virological remission after the interruption of early initiated antiretroviral therapy ANRS VISCONTI Study. *PLoS Pathog.* **9**, e1003211 (2013).
13. G. Namazi *et al.*, The control of HIV after antiretroviral medication pause (CHAMP) study: Post-treatment controllers identified from 14 clinical studies. *J. Infect. Dis.* **218**, 1954–1963 (2018).
14. A. A. Bashirova *et al.*, LILRB2 interaction with HLA class I correlates with control of HIV-1 infection. *PLoS Genet.* **10**, e1004196 (2014).
15. K. M. Bruner *et al.*, A quantitative approach for measuring the reservoir of latent HIV-1 proviruses. *Nature* **566**, 120–125 (2019).
16. Y. C. Ho *et al.*, Replication-competent noninduced proviruses in the latent reservoir increase barrier to HIV-1 cure. *Cell* **155**, 540–551 (2013).
17. K. J. Kwon *et al.*, Different human resting memory CD4(+) T cell subsets show similar low inducibility of latent HIV-1 proviruses. *Sci. Trans. Med.* **12**, eaax6795 (2020).
18. L. Zheng *et al.*, Factors associated with CD8+ T-cell activation in HIV-1-infected patients on long-term antiretroviral therapy. *J. Acquir. Immune. Defic. Syndr.* **67**, 153–160 (2014).
19. G. Khoury *et al.*, Human immunodeficiency virus persistence and T-cell activation in blood, rectal, and lymph node tissue in human immunodeficiency virus-infected individuals receiving suppressive antiretroviral therapy. *J. Infect. Dis.* **215**, 911–919 (2017).
20. M. Pino *et al.*, Increased homeostatic cytokines and stability of HIV-infected memory CD4 T-cells identify individuals with suboptimal CD4 T-cell recovery on-ART. *PLoS Pathog.* **17**, e1009825 (2021).
21. B. A. Peters *et al.*, T-cell immune dysregulation and mortality in women with human immunodeficiency virus. *J. Infect. Dis.* **225**, 675–685 (2022).
22. M. Helleberg *et al.*, Course and clinical significance of CD8+ T-cell counts in a large cohort of HIV-infected individuals. *J. Infect. Dis.* **211**, 1726–1734 (2015).
23. S. Serrano-Villar *et al.*, HIV-infected individuals with low CD4/CD8 ratio despite effective antiretroviral therapy exhibit altered T cell subsets, heightened CD8+ T cell activation, and increased risk of non-AIDS morbidity and mortality. *PLoS Pathog.* **10**, e1004078 (2014).

24. B. Youngblood *et al.*, Cutting edge: Prolonged exposure to HIV reinforces a poised epigenetic program for PD-1 expression in virus-specific CD8 T cells. *J. Immunol.* **191**, 540–544 (2013).
25. K. B. Yates *et al.*, Epigenetic scars of CD8(+) T cell exhaustion persist after cure of chronic infection in humans. *Nat. Immunol.* **22**, 1020–1029 (2021).
26. G. D. Gaiha *et al.*, Structural topology defines protective CD8(+) T cell epitopes in the HIV proteome. *Science* **364**, 480–484 (2019).
27. D. Z. Soghoian *et al.*, HIV-specific cytolytic CD4 T cell responses during acute HIV infection predict disease outcome. *Sci. Trans. Med.* **4**, 123ra125 (2012).
28. D. C. Douek *et al.*, HIV preferentially infects HIV-specific CD4+ T cells. *Nature* **417**, 95–98 (2002).
29. D. R. Collins *et al.*, Functional impairment of HIV-specific CD8(+) T cells precedes aborted spontaneous control of viremial. *Immunity* **54**, 2372–2384.e2377 (2021).
30. V. A. Vieira *et al.*, Robust HIV-specific CD4+ and CD8+ T-cell responses distinguish elite control in adolescents living with HIV from viremic nonprogressors. *Aids* **36**, 95–105 (2022).
31. J. E. McKinnon *et al.*, Baseline natural killer and T cell populations correlation with virologic outcome after regimen simplification to atazanavir/ritonavir alone (ACTG 5201). *PLoS One* **9**, e95524 (2014).
32. J. T. Kim *et al.*, Latency reversal plus natural killer cells diminish HIV reservoir in vivo. *Nat. Commun.* **13**, 121 (2022).
33. M. M. Lederman, N. T. Funderburg, R. P. Sekaly, N. R. Klatt, P. W. Hunt, Residual immune dysregulation syndrome in treated HIV infection. *Adv. Immunol.* **119**, 51–83 (2013).
34. K.-A. Lê Cao, S. Boitard, P. Besse, Sparse PLS discriminant analysis: Biologically relevant feature selection and graphical displays for multiclass problems. *BMC Bioinformatics* **12**, 253 (2011).
35. J. P. Williams *et al.*, HIV-1 DNA predicts disease progression and post-treatment virological control. *Elife* **3**, e03821 (2014).
36. L. Assoumou, A low HIV-DNA level in PBMCs at antiretroviral treatment interruption predicts a higher probability of maintaining viral control. *AIDS* **29**, 2003–2007 (2015).
37. J. Blazkova *et al.*, Distinct mechanisms of long-term virologic control in two HIV-infected individuals after treatment interruption of anti-retroviral therapy. *Nat. Med.* **27**, 1893–1898 (2021).
38. A. Wedrychowski *et al.*, Transcriptomic signatures of human immunodeficiency virus post-treatment control. *J. Virol.* **97**, e0125422 (2022).
39. C. Gálvez *et al.*, Atlas of the HIV-1 reservoir in peripheral CD4 T cells of individuals on successful antiretroviral therapy. *mBio* **12**, e0307821 (2021).
40. A. L. Meditz *et al.*, HLA-DR+ CD38+ CD4+ T lymphocytes have elevated CCR5 expression and produce the majority of R5-tropic HIV-1 RNA in vivo. *J. Virol.* **85**, 10189–10200 (2011).
41. H. Hatano *et al.*, Cell-based measures of viral persistence are associated with immune activation and programmed cell death protein 1 (PD-1)-expressing CD4+ T cells. *J. Infect. Dis.* **208**, 50–56 (2013).
42. P. W. Hunt *et al.*, Relationship between T cell activation and CD4+ T cell count in HIV-seropositive individuals with undetectable plasma HIV RNA levels in the absence of therapy. *J. Infect. Dis.* **197**, 126–133 (2008).
43. J. Z. Li *et al.*, Antiretroviral therapy reduces T-cell activation and immune exhaustion markers in human immunodeficiency virus controllers. *Clin. Infect. Dis.* **70**, 1636–1642 (2020).
44. J. Z. Li *et al.*, Differential levels of soluble inflammatory markers by human immunodeficiency virus controller status and demographics. *Open Forum. Infect. Dis.* **2**, ofu117 (2015).
45. A. Cozzi-Lepri *et al.*, Resumption of HIV replication is associated with monocyte/macrophage derived cytokine and chemokine changes: results from a large international clinical trial. *AIDS* **25**, 1207–1217 (2011).
46. S. M. Keating *et al.*, The effect of HIV infection and HAART on inflammatory biomarkers in a population-based cohort of women. *AIDS* **25**, 1823–1832 (2011).
47. A. Kamat *et al.*, A plasma biomarker signature of immune activation in HIV patients on antiretroviral therapy. *PLoS One* **7**, e30881 (2012).
48. T. H. Burdo *et al.*, Soluble CD163 made by monocyte/macrophages is a novel marker of HIV activity in early and chronic infection prior to and after anti-retroviral therapy. *J. Infect. Dis.* **204**, 154–163 (2011).
49. T. H. Burdo *et al.*, Soluble CD163, a novel marker of activated macrophages, is elevated and associated with noncalcified coronary plaque in HIV-infected patients. *J. Infect. Dis.* **204**, 1227–1236 (2011).
50. F. Pereyra *et al.*, Increased coronary atherosclerosis and immune activation in HIV-1 elite controllers. *AIDS* **26**, 2409–2412 (2012).
51. S. Subramanian *et al.*, Arterial inflammation in patients with HIV. *JAMA* **308**, 379–386 (2012).
52. W. M. El-Sadr *et al.*, CD4+ count-guided interruption of antiretroviral treatment. *N. Engl. J. Med.* **355**, 2283–2296 (2006).
53. M. R. Betts *et al.*, HIV nonprogressors preferentially maintain highly functional HIV-specific CD8+ T cells. *Blood* **107**, 4781–4789 (2006).
54. R. T. Schooley *et al.*, AIDS clinical trials group 5197: A placebo-controlled trial of immunization of HIV-1-infected persons with a replication-deficient adenovirus type 5 vaccine expressing the HIV-1 core protein. *J. Infect. Dis.* **202**, 705–716 (2010).
55. G. Alter *et al.*, Differential natural killer cell-mediated inhibition of HIV-1 replication based on distinct KIR/HLA subtypes. *J. Exp. Med.* **204**, 3027–3036 (2007).
56. V. D. Gonzalez *et al.*, Expansion of functionally skewed CD56-negative NK cells in chronic hepatitis C virus infection: Correlation with outcome of pegylated IFN-α and ribavirin treatment. *J. Immunol.* **183**, 6612–6618 (2009).
57. F. Marras *et al.*, Natural killer cells in HIV controller patients express an activated effector phenotype and do not up-regulate NKp44 on IL-2 stimulation. *Proc. Natl. Acad. Sci. U.S.A.* **110**, 11970–11975 (2013).
58. A. F. George *et al.*, Deep phenotypic analysis of blood and lymphoid T and NK cells from HIV+ controllers and ART-suppressed individuals. *Front. Immunol.* **13**, 803417 (2022).
59. V. A. Vieira *et al.*, An HLA-I signature favouring KIR-educated natural killer cells mediates immune control of HIV in children and contrasts with the HLA-B-restricted CD8+ T-cell-mediated immune control in adults. *PLOS Pathog.* **17**, e1010090 (2021).
60. Y. C. Bartsch *et al.*, Viral rebound kinetics correlate with distinct HIV antibody features. *mBio* **12**, e00170-21 (2021).
61. D. Scott-Algara, "Post-treatment controllers have particular NK cells with high anti-HIV capacity: VISCONTI study" in *22nd Conference on Retroviruses and Opportunistic Infections (CROI 2015)*, (Accessed 1 January 2023).
62. C. Jiang *et al.*, Distinct viral reservoirs in individuals with spontaneous control of HIV-1. *Nature* **585**, 261–267 (2020).
63. X. Lian *et al.*, Signatures of immune selection in intact and defective proviruses distinguish HIV-1 elite controllers. *Sci. Trans. Med.* **13**, eabl4097 (2021).
64. K. B. Einkauf *et al.*, Parallel analysis of transcription, integration, and sequence of single HIV-1 proviruses. *Cell* **185**, 266–282.e215 (2022).
65. P. Volberding *et al.*, Antiretroviral therapy in acute and recent HIV infection: A prospective multicenter stratified trial of intentionally interrupted treatment. *AIDS* **23**, 1987–1995 (2009).
66. J. M. Kilby *et al.*, A randomized, partially blinded phase 2 trial of antiretroviral therapy, HIV-specific immunizations, and interleukin-2 cycles to promote efficient control of viral replication (ACTG A5024). *J. Infect. Dis.* **194**, 1672–1676 (2006).
67. J. M. Jacobson *et al.*, Evidence that intermittent structured treatment interruption, but not immunization with ALVAC-HIV vCP1452, promotes host control of HIV replication: The results of AIDS Clinical Trials Group 5068. *J. Infect. Dis.* **194**, 623–632 (2006).
68. K. Henry *et al.*, A pilot study evaluating time to CD4 T-cell count <350 cells/mm(3) after treatment interruption following antiretroviral therapy +/- interleukin 2: Results of ACTG A5102. *J. Acquir. Immune. Defic. Syndr.* **42**, 140–148 (2006).
69. R. T. Gandhi *et al.*, A randomized therapeutic vaccine trial of canarypox-HIV-pulsed dendritic cells vs. canarypox-HIV alone in HIV-1-infected patients on antiretroviral therapy. *Vaccine* **27**, 6088–6094 (2009).
70. D. J. Skiest *et al.*, Interruption of antiretroviral treatment in HIV-infected patients with preserved immune function is associated with a low rate of clinical progression: A prospective study by AIDS Clinical Trials Group 5170. *J. Infect. Dis.* **195**, 1426–1436 (2007).
71. E. S. Rosenberg *et al.*, Safety and immunogenicity of therapeutic DNA vaccination in individuals treated with antiretroviral therapy during acute/early HIV-1 infection. *PLoS One* **5**, e10555 (2010).
72. M. S. Malnati *et al.*, A universal real-time PCR assay for the quantification of group-M HIV-1 proviral load. *Nat. Protoc.* **3**, 1240–1248 (2008).
73. C. Ledderose, J. Heyn, E. Limbeck, S. Kreth, Selection of reliable reference genes for quantitative real-time PCR in human T cells and neutrophils. *BMC Res. Notes* **4**, 427 (2011).
74. Y. J. Park *et al.*, Impact of HLA class I alleles on timing of HIV rebound after antiretroviral treatment interruption. *Pathog. Immun.* **2**, 431–445 (2017).
75. S. Vardhanabhuti *et al.*, Clinical and genetic determinants of plasma nevirapine exposure following an intrapartum dose to prevent mother-to-child HIV transmission. *J. Infect. Dis.* **208**, 662–671 (2013).
76. R. P. van Heeswijk *et al.*, The steady-state pharmacokinetics of nevirapine during once daily and twice daily dosing in HIV-1-infected individuals. *AIDS* **14**, F77–82 (2000).
77. G. Moyle *et al.*, Steady-state pharmacokinetics of abacavir in plasma and intracellular carbovir triphosphate following administration of abacavir at 600 milligrams once daily and 300 milligrams twice daily in human immunodeficiency virus-infected subjects. *Antimicrob. Agents Chemother.* **53**, 1532–1538 (2009).
78. L. J. Else *et al.*, Pharmacokinetics of lamivudine and lamivudine-triphosphate after administration of 300 milligrams and 150 milligrams once daily to healthy volunteers: Results of the ENCORE 2 study. *Antimicrob. Agents Chemother.* **56**, 1427–1433 (2011).